Femtosecond control of electronic motion in semiconductor double quantum wells

A. Matos-Abiague and J. Berakdar
Max-Planck Institut für Mikrostrukturphysik, Weinberg 2, 06120 Halle, Germany
(Received 21 November 2003; published 1 April 2004)

A presently realizable picosecond half-cycle electromagnetic pulse (HCP) consists of a short (<1 ps) unipolar part followed by a long (~ 100 ps), much weaker unipolar part of opposite polarity. In this work we investigate the quantum dynamics and emission properties of an electron driven by a train of HCP's in a $Al_xGa_{1-x}As$ based symmetric double quantum well. Our full numerical results, analyzed with the aid of a simple analytical model, show that an appropriately designed train of HCP's allows the coherent control of the electron motion on a subpicosecond scale, i.e., the electron can be driven to achieve and maintain a predefined final state for hundreds of picoseconds. We further show that it is possible to engineer the emission spectrum by an appropriate choice of the HCP's parameters. Consequences of the absence of the generalized parity of the Floquet modes on the dynamics of the system are discussed. Phenomena such as coherent suppression of tunneling in the absence of accidental degeneration of quasienergies, low-frequency generation, and half-harmonic generation are observed. An estimate of the pulse parameters that allows the efficient control of the electron motion and its emission spectrum are derived from a simplified analytical model.

DOI: 10.1103/PhysRevB.69.155304 PACS number(s): 73.40.Gk, 42.65.Re, 02.30.Yy, 85.35.Be

I. INTRODUCTION

The study of the electron quantum dynamics in quantum well structures under external time-dependent driving has revealed a variety of novel phenomena. Here we mention, in particular, the coherent suppression of tunneling[1,2] and the low-frequency generation[2] in a symmetric double quantum well under the influence of a continuous-wave (cw) laser as well as the possibility to coherently control the quantum dynamics by appropriate shaping of the driving field properties. Based on these findings various ideas for applications have been put forward, such as the laser-induced trapping of an electron in a quantum well,[2] the control of electron transfer reactions,[3] the stabilization of a given configuration of an atom or molecule,[4–8] and the creation of entangled states.[9] The coherent control is also highly desirable for potential applications in designing electro-optical devices and is essential for the realization of quantum computation.

For *periodic* (cw) driving fields, the coherence properties and the quantum dynamics in double-well potentials[1,2,10] and in two-level systems[1,10–14] have been explored theoretically in considerable details. On the other hand during recent years new development in shaping electromagnetic pulses render possible the generation and controlled manipulation of so-called half-cycle pulses (HCP's) (Ref. 4) in the subpicosecond regime. A HCP acts as a unipolar electromagnetic pulse. In fact, for a freely propagating electromagnetic wave Maxwell's equations require a vanishing time integral over the electric field. Therefore, a HCP is strictly speaking a strongly asymmetric monocycle pulse that is composed of a very short, strong half-cycle (only this part is usually relevant for the dynamics and is referred to as a HCP), followed by a much slower half cycle of an opposite polarity and a much weaker amplitude (this part is called the tail of the pulse). Typical pulse amplitude asymmetry is 13:1.[4] The tail of the HCP acts, on the time scale of the electron dynamics, as a weak offset dc field that hardly affects the electron motion (this we checked numerically for the results shown below).

The influence of cw lasers and HCP's on the electron dynamics is then qualitatively different. As demonstrated by a number of studies, in case of a monochromatic cw laser only the characteristic frequency of the laser is relevant.[1,2,10–13] In contrast, HCP's deliver a wide range of frequencies to the system. In addition, if the characteristic time of the electron motion in the the absence of the driving field (e.g., the round-trip time of a confined electron) is much longer than the duration of the HCP, the electron-HCP interaction can be viewed classically as an impulsive ''kick'' received by the electron.[6,15,16] The strength of the kick, i.e., of the momentum change, is determined by $\mathbf{\Delta p}=-\int \mathbf{F}(t)dt$. Here $\mathbf{F}(t)$ is the time-dependent field of the HCP. Quantum mechanically, the influence of an HCP on the electron can be described as a linear transformation of the momentum space wave function in the direction of the kick, $\tilde{\Psi}(\mathbf{p})\rightarrow\tilde{\Psi}(\mathbf{p}+\mathbf{\Delta p})$. In configuration space we can view the action of the HCP on the electron as a phase shift of the electron wave function in the following way: $\Psi(\mathbf{r})\rightarrow\Psi(\mathbf{r})e^{-i\mathbf{\Delta p}\cdot\mathbf{r}}$. In view of these fundamental differences between cw and HCP's driving it is useful and timely to consider the possibility of controlling on the *subpicosecond* scale the motion of an electron confined in a $Al_xGa_{1-x}As$ based double quantum well, a phenomenon that could be useful in designing ultrafast switches or for the construction and control of quantum logic states (e.g., one can associate 1 and 0 with the states in which the electron is localized in the left and in the right well, respectively). Below we utilize a conveniently designed train of ultrashort half-cycle pulses. Although the full control in designing electromagnetic pulses still constitutes a challenge for experimentalists, an enormous progress has been achieved recently. Laser techniques available nowadays allow the generation of electromagnetic pulses with durations in the femtosecond[17] or even in the attosecond[18] regimes. HCP's with a peak field up to hundreds of kV/cm and duration in the subpicosecond regime are currently available[4,15] and new principles for generation of unipolar pulses as short as 0.1 fs and with intensities up to 10^{16} W/cm^2 have recently

been proposed.[19] Techniques for sampling HCP's[20] and for creating trains of ultrashort HCP's are also available nowadays.[5,6] These techniques allow a fine control of the time delay between consecutive pulses. In particular, trains of HCP's have been employed in the experimental study of the ionization and dynamical stabilization of Rydberg atoms.[5,6]

The key finding of the present study is that an appropriately designed train of HCP's renders possible the femtosecond control of the electron motion in symmetric quantum wells (in contrast, such a process lasts several picoseconds when cw lasers are used as driving fields[2]). The emission spectrum of the system can also be selectively designed. Furthermore, it is shown that, contrary to the case of cw lasers as driving fields, when HCP's are used the control process is robust to appreciable changes in the parameters of the driving field.

II. GENERAL FORMULATION

We consider a conduction electron confined in a typical $Al_xGa_{1-x}As$ based double quantum well. Within the parabolic band and the effective-mass approximations, the time-dependent Schrödinger equation describing the dynamics of the system under a train of HCP's can be written as

$$i\hbar\frac{\partial\Psi}{\partial t}=H\Psi, \quad H=H_0+V_{\text{conf}}+V(z,t), \tag{1}$$

where H_0 represents the bare Hamiltonian, V_{conf} refers to the double-well confinement potential, and $V(z,t)$ stands for the interaction of the electron with the pulses. We employ in the present work a symmetric shape for the confinement potential similar to that used in Ref. 2. The central barrier height is about 240 meV and the wells and central barrier widths are, approximately, 50 Å and 60 Å, respectively. The electron effective mass $m^*=0.067m_0$ is assumed constant through the heterostructure. For the phenomena studied in this work, effects of elastic scattering and electron-phonon interaction are subsidiary. The reason lies in the different time scales: As demonstrated explicitly below, HCP's-driven localization of the electron wave packet is achieved on the femtosecond scale. On the other hand, for typical electron concentrations in high quality Ga(Al)As-GaAs heterostructures elastic scattering and electron-phonon interaction occur on the scale of several picoseconds,[21] i.e., these processes are too slow to be able to affect the localization process.

The electron interaction with the train of strongly asymmetric pulses can be described by the potential

$$V(z,t)=z\sum_{k=0}^{N-1}F_kU(t-t_p-kT), \tag{2}$$

where

$$U(t)=\begin{cases}\exp\left[-\dfrac{t^2}{2\sigma^2}\right]\cos\Omega t & \text{if} -\dfrac{\pi}{2\Omega}\leqslant t<T-\dfrac{\pi}{2\Omega}\\ 0 \quad \text{otherwise.}\end{cases} \tag{3}$$

In Eqs. (2) and (3) F_k denotes the peak field of the kth pulse, $t_p=\pi/(2\Omega)$ corresponds to the time at which the positive tail of the first applied pulse is centered, T is the time between consecutive pulses, N is the number of applied pulses, and σ characterizes the width of the pulses. The parameter $\Omega=\pi/(3\sigma\sqrt{\ln 2})$ in Eq. (3) guarantees a ratio 8:1 between the peak amplitudes of the positive and negative parts of the pulses. The duration d of the positive part of each pulse (i.e., of the HCP's) is given by $d=3\sigma\sqrt{\ln 2}$.

A. Numerical model

The time-dependent Schrödinger equation [Eq. (1)] cannot be solved analytically, we therefore implemented a fast-Fourier-transform based numerical method as described in (Ref. 22) for the propagation of the initial wave function in time. After computation of the time-dependent wave function $\Psi(x,t)$, we calculated the time-dependent probability

$$P_L(t)=\int_{-\infty}^{0}\Psi^*(x,t)\Psi(x,t)dx. \tag{4}$$

The time-averaged probability

$$\langle P_L\rangle_\tau=\frac{1}{\tau}\int_0^\tau P_L(t)dt, \tag{5}$$

we use as a measure for finding the electron in the left well. The emission properties are studied through the quantity

$$I(\omega)=\left|\int_{-\infty}^{\infty}\mu(t)\exp[-i\omega t]dt\right|, \tag{6}$$

where $\mu(t)=\langle\Psi(z,t)|z|\Psi(z,t)\rangle$ is the time-dependent dipole moment. All calculations were performed with $\sigma=20$ fs and $T=100$ fs.

B. Analytical approach

For a better understanding of dependencies of the electron motion on the various parameters of the pulses we developed, in addition to the numerical scheme, a simple analytical approach that is capable of reproducing and explaining the main features of the numerical calculations. The analytical model is based on the observation that for the system under study the two lowest-energy levels are well separated from the other energy states. Hence, for a certain range of pulse parameters the system will behave, basically, as a two-level system. Although, the two-level system approximation (TLSA) introduces certain simplifications, the corresponding time-dependent Schrödinger equation with the interaction potential in Eq. (2) cannot be solved analytically. However, further simplification is brought about by the fact that for ultrashort HCP's the duration of each pulse is much smaller than the typical characteristic time T_c of the undriven system (in the double quantum well studied here, we have, for example, $T_c\approx 665$ fs in the absence of the pulses, while the duration of the employed pulses is about 80 fs). As the width of the pulses is very small compared to the characteristic time of the undriven system, one can apply the sudden approximation (SA). As outlined in the Introduction, the SA

amounts to replacing the kth pulse by an instantaneous kick that results in the momentum transfer

$$\Delta p_k = \int_{-\pi/2\Omega}^{T-\pi/2\Omega} F_k U(t)dt \tag{7}$$

to the system.[6,15,16] The electron-pulses interaction can then be approximated as

$$V(z,t) \approx z \sum_{k=0}^{N-1} \Delta p_k \delta(t - t_p - kT), \tag{8}$$

where $\delta(x)$ represents the Dirac delta function. Note that the kth kick is applied at the time when the original kth pulse reaches its maximum amplitude. Hence, the actual train of pulses [Eq. (2)] starts at $t=0$, while within the SA the HCP's sequence [Eq. (8)] starts at $t=t_p$. For the sake of generality, in what follows we will denote by t_0 the time at which the train of pulses is turned on (i.e., $t_0=0$ for the exact calculation and $t_0=t_p$ for the analytical approach). Where confusion may occur we specify explicitly the particular value of t_0.

Within the TLSA the wave function of the system can be expressed as

$$\Psi(z,t) = \sum_{n=1}^{2} C_n(t) \Psi_n^{(0)}(x), \tag{9}$$

where $\Psi_n^{(0)}(x)(n=1,2)$ represent the two lowest levels of the field-free system. The expansion coefficients $C_n(t)$ define a two-dimensional spinor $\mathbf{C}(t)=(C_1(t),C_2(t))^T$. For our purpose it is convenient to perform a transformation from the spinor space to the real space. It can be done through a transition from SU(2) to SO(3) by introducing the Bloch vector $\mathbf{B}=(B_x,B_y,B_z)$ whose components are given by

$$B_i = \mathbf{C}^\dagger \sigma_i \mathbf{C}, \quad i=x,y,z, \tag{10}$$

where σ_i represent the Pauli matrices. The evolution of the system is then described by rotations of the real vector $\mathbf{B}$ with the constraint $|\mathbf{B}|=1$ imposed by the normalization of the wave function.

From Eqs. (1), (8)–(10) one obtains, after the corresponding time integration, that the action of the kth pulse on the system is determined, in the Bloch space, by the following relation:

$$\mathbf{B}(t_k) = \begin{pmatrix} 1 & 0 & 0 \\ 0 & \cos\alpha_k & \sin\alpha_k \\ 0 & -\sin\alpha_k & \cos\alpha_k \end{pmatrix} \mathbf{B}(t_k^-), \tag{11}$$

where

$$\alpha_k = \frac{2\mu_{12}\Delta p_k}{\hbar}, \tag{12}$$

μ_{12} is the dipole corresponding to transitions between the two lowest eigenstates of the unperturbed system, and $t_k^- = t_k - \epsilon$ (with $\epsilon \to 0^+$) and t_k refer to the times just before and right after the kth pulse, respectively. On the other hand the field-free evolution of the system in the time intervals $t_k \leqslant t < t_{k+1}$ is determined by

$$\mathbf{B}(t) = \begin{pmatrix} \cos\beta_k & -\sin\beta_k & 0 \\ \sin\beta_k & \cos\beta_k & 0 \\ 0 & 0 & 1 \end{pmatrix} \mathbf{B}(t_k), \tag{13}$$

where

$$\beta_k = \frac{2\pi(t-t_k)}{T_c}. \tag{14}$$

The probability $P_L(t)$ of finding the electron in the left well can be written, in terms of the Bloch vector, as follows:

$$P_L(t) = \frac{1+B_x(t)}{2}, \tag{15}$$

while the time-dependent dipole reads as

$$\mu(t) = \mu_{12} B_x(t). \tag{16}$$

Equations (15) and (16) lead to

$$\mu(t) = \mu_{12}[2P_L(t)-1]. \tag{17}$$

This expression relates the dynamics of the electron motion [characterized by $P_L(t)$] to its emission properties [characterized by the Fourier transform of $\mu(t)$].

In the case of a quasiperiodic train of pulses, the study of the properties of the Floquet states and their quasienergies is of particular interest for understanding the dynamics of the system as well as its emission spectrum. Within the Floquet theory, the wave function of the system can be expanded in Floquet states $\Psi_\lambda(z,t)$ as[10]

$$\Psi(z,t) = \sum_\lambda A_\lambda \Psi_\lambda(z,t), \tag{18}$$

where

$$\Psi_\lambda(z,t) = e^{-i\varepsilon_\lambda t/\hbar} \Phi_\lambda(z,t). \tag{19}$$

The substitution of Eqs. (18) and (19) in Eq. (1) leads to the following eigenvalue problem:[10]

$$\left[H - i\hbar \frac{\partial}{\partial t} \right] \Phi_\lambda(z,t) = \varepsilon_\lambda \Phi_\lambda(z,t), \tag{20}$$

for determining the Floquet modes Φ_λ (eigenfunctions) and their corresponding quasienergies ε_λ (eigenvalues). Unlike the wave function $\Psi(z,t)$, the Floquet modes $\Phi_\lambda(z,t)$ are periodic, i.e., $\Phi_\lambda(z,t)=\Phi_\lambda(z,t+T)$. This periodicity can be exploited to obtain the Floquet modes at stroboscopic times ($t=t_0+kT$, $k=0,1,2,\ldots$) and the corresponding quasienergies from the eigenfuntions and eigenvalues, respectively, of the evolution operator over one period, i.e.,

$$U(t_0+T,t_0)\Phi_\lambda(t_0) = e^{-i\varepsilon_\lambda T/\hbar} \Phi_\lambda(t_0), \tag{21}$$

where $U(t_0+T,t_0)$ represents the evolution operator from $t=t_0$ to $t=t_0+T$.

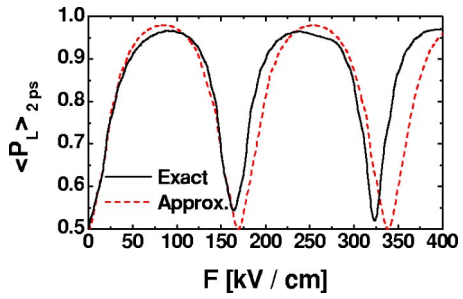

FIG. 1. (Color online) Time average of P_L as a function of the pulse strength for tunneling initial condition.

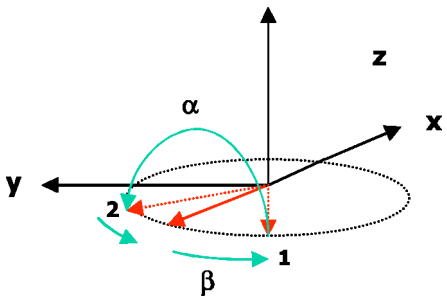

FIG. 2. (Color online) Geometrical interpretation of the localization condition, Eq. (24).

It is worth noting that, in contrast to the case of a cw laser, for HCP's Eq. (20) is not invariant under the transformations $z\rightarrow -z; t\rightarrow t+T/2$. Consequently, the Floquet modes $\Phi_\lambda(z,t)$ do not have well-defined generalized parity. In such a situation one can conclude, based on the von Neumann–Wigner theorem,[23] that the existence of exact quasienergy crossings in the space of system parameters is no longer guaranteed and the quasienergies exhibit typically avoided crossings.

Within the TLSA and the SA, the quasienergies were found to be given by

$$\varepsilon_\lambda = \epsilon_l + n\hbar\omega_0, \tag{22}$$

where $\lambda=(l,n)(l=1,2;\ n=0,\pm 1,\pm 2,\ldots)$ and

$$\epsilon_1 = -\frac{\hbar\omega_0}{2\pi}\arccos(\cos\varphi\cos\vartheta); \quad \epsilon_2 = -\epsilon_1, \tag{23}$$

with $\varphi=\mu_{12}\Delta p/\hbar$ and $\vartheta=\pi\omega_c/\omega_0$ ($\omega_c=2\pi/T_c$ is the characteristic frequency of the field-free system and $\omega_0=2\pi/T$ is the frequency corresponding to the train of pulses).

III. RESULTS

As the evolution of the wave function strongly depends on the initial conditions, we consider two possibilities for the initial wave function corresponding to initially localized (tunneling initial condition) and initially delocalized (optical initial condition) states.

A. Tunneling initial condition

In this case we consider an electron whose state at $t=0$ is given by $|\Psi_0\rangle=(|1\rangle-|2\rangle)/\sqrt{2}$, where $|1\rangle$ and $|2\rangle$ are the two lowest-energy eigenstates of the electron in the absence of the pulses. This case corresponds to a particle trapped initially in the left well. As in this case the coherent suppression of tunneling leads to the maintenance of the localization of the electron in the left well, in what follows we will refer to the coherent suppression of tunneling just as *localization*.

1. Wave-function localization

The dependence of the average probability $\langle P_L\rangle$ of finding the electron in the left well on the pulse strength is displayed in Fig. 1 for the case of a quasiperiodic train of HCP's. The solid and dashed lines correspond to the full numerical calculation (including all the levels) and the analytical approximation, respectively. A good agreement between both calculations is found in the region of small pulse amplitudes. For strong pulses more than two levels are involved in the dynamic's of the system and the TLSA is no longer valid. In this case the differences between the analytical model and the exact numerical results become more prevalent.

A remarkable fact is that, contrary to the case of a cw laser as a driving field, a train of HCP's can maintain the localization of the initially trapped particle in a wide range of pulse parameters. The existence of certain pulse amplitudes leading to optimal localization and delocalization can also be appreciated in Fig. 1. This behavior can be explained (within the analytical approximation) from the geometrical interpretation of the dynamics of the system in the Bloch space. In the Bloch space the tunneling initial condition is represented by the vector $(-1,0,0)$. Before applying the first pulse, the vector **B** rotates counterclockwise around the z axis until the first pulse is applied at $t=t_p$. Just before the first kick, the vector **B** has then rotated an angle $\beta=2\pi t_p/T_c$ (see position 1 in Fig. 2). The first kick induces a rotation of **B** around the x axis. If the angle α of the kick-induced rotation is

$$\alpha = \frac{2\mu_{12}\Delta p}{\hbar} = (2n+1)\pi \quad (n\in\mathcal{Z}), \tag{24}$$

then after the kick the vector **B** will be at position 2 (see Fig. 2), i.e., before the first pulse the particle was leaving the left well and now, after the pulse, the particle is returning to that well. If this procedure is iterated with $T<T_c/4$ the vector **B** will remain oscillating in the vicinity of $(-1,0,0)$, i.e., the particle will remain localized to a large extent in the left well. This situation corresponds to a quasiperiodic cyclic evolution of the Bloch vector [in general, $\mathbf{B}(t_p+2kT)=\mathbf{B}(t_p)$ and in the particular case $T=2t_p$ then $\mathbf{B}(t_p+kT)=\mathbf{B}(t_p)$]. Therefore, we can conclude that iterated (or quasiperiodic in the case of a time quasiperiodic external field) cyclic evolution can be regarded as a *necessary* condition for achievement of sustainable (i.e., can be sustained for a time interval longer than the characteristic time of the unperturbed system) localization. Note, however, that the existence of quasiperiodic cyclic evolution is not sufficient for achieving localization. For this to happen, it is also necessary that the particle does not delocalize during one evolution cycle.

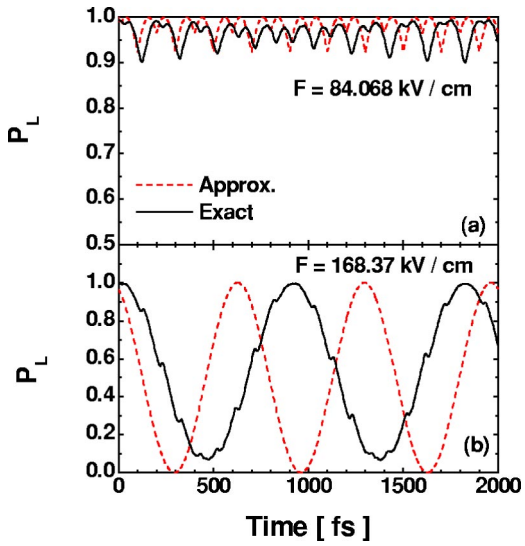

FIG. 3. (Color online) *Tunneling initial condition*. (a) Time dependence of P_L for a pulse amplitude corresponding to $n=0$ in the localization condition, Eq. (24). (b) Same as in (a) but for a pulse amplitude corresponding to $n=1$ in the delocalization condition, Eq. (25).

Therefore, if $T<T_c/4$ (this condition prevents the delocalization of the particle during an evolution cycle), Eq. (24) represents a condition for determining the pulse parameters leading to the optimization of the electron localization in the left well. This behavior is illustrated in Fig. 3(a), where the time dependence of the probability P_L of finding the electron in the left well is displayed for a pulse amplitude $F=84.068$ kV/cm corresponding to $n=0$ in Eq. (24). Solid and dashed lines correspond to the exact numerical calculations and to the analytical approximation, respectively (we stress that the exact numerical calculation is not a two-level system calculation but a full numerical solution of the Schrödinger equation, including all the levels of the system). If, on the contrary, the parameters of the pulse are such that

$$\alpha=\frac{2\mu_{12}\Delta p}{\hbar}=2n\pi \quad (n\in\mathcal{Z}), \tag{25}$$

then after the pulse the vector **B** returns to position 1 (see Fig. 2), i.e., in this case the particle does not feel the field and behaves as in the field-free case, oscillating from one well to the other with a period approximately equal to the characteristic time of the unperturbed system. This situation is shown in Fig. 3(b), where the probability of remaining in the left well as a function of time is shown for a pulse amplitude $F=168.37$ kV/cm that corresponds to the case $n=1$ in Eq. (25).

The dependence of the quasienergies (calculated within the analytical approximation) on the pulse strength is displayed in Fig. 4, showing that for the system studied here no crossing (and, therefore, no accidental degeneration) of quasienergies occurs. This situation, as mentioned in the preceding section, is a consequence of the lack of well-defined generalized parity of the Floquet modes.

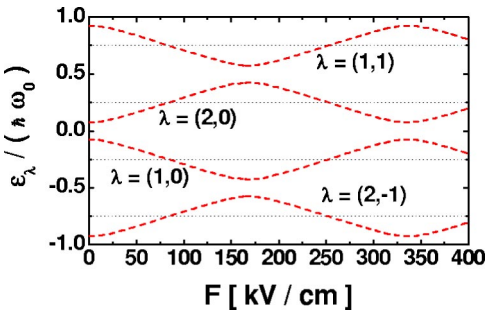

FIG. 4. (Color online) Dependence of the quasienergies on the pulse amplitude.

The existence of localization in the absence of accidental degeneration of the quasienergies may appear surprising at first sight, since the existence of quasienergy crossings in the system parameter space is usually regarded as a necessary condition for the achievement of coherent suppression of tunneling.[1,2,10,11] However, as discussed before, the actual necessary condition for inducing a sustainable localization by a quasiperiodic external field is the requirement of quasiperiodic cyclic evolution of the wave function of the system and, as will be explained bellow, the existence of accidental degeneration of the quasienergies is not the only mechanism that can lead to quasiperiodic cyclic evolution.

The quasiperiodic cyclic evolution corresponding to a system, that is, in a known *initial* state at the time the external time-quasi-periodic perturbation is switched on (i.e., at $t=t_0$) can be mathematically expressed as

$$\Psi(z,t_0+k\mathcal{T})=e^{i\phi_k}\Psi(z,t_0), \quad k=0,1,2,\ldots, \tag{26}$$

where ϕ_k is a real number and $\mathcal{T}$ represents the duration of one evolution cycle (note that $\mathcal{T}$ does not necessarily coincide with T). Equation (26) together with the requirement $\mathcal{T}<\tau_{\mathrm{del}}$ (with τ_{del} the delocalization time of the perturbed system) can then be regarded as the necessary and sufficient conditions for achieving dynamical localization.

Taking into account the periodicity of the Floquet modes, Eq. (18) can be written (within the TLSA) as

$$\begin{aligned}\Psi(z,t_0+kT)=&\exp\left(-i\frac{\epsilon_2 kT}{\hbar}\right)\\ &\times[e^{-ikT(\epsilon_1-\epsilon_2)/\hbar}A_1e^{-it_0\epsilon_1/\hbar}\Phi_1(z,t_0)\\ &+A_2e^{-it_0\epsilon_2/\hbar}\Phi_2(z,t_0)].\end{aligned} \tag{27}$$

One can see that Eq. (27) can be reduced to Eq. (26) if one of the following three conditions is fulfilled.

(a) If $\epsilon_1-\epsilon_2=n\hbar\omega_0$ $(n\in\mathcal{Z})$.

(b) If $A_1=0$ or $A_2=0$.

(c) If $\epsilon_1-\epsilon_2=\hbar\omega_0/m+n\hbar\omega_0$ $(m,n\in\mathcal{Z};\ m\neq\pm1)$.

The condition (a) corresponds to degeneration of the quasienergies and leads to $\mathcal{T}=T$. The conditions (b) and (c) lead to $\mathcal{T}=T$ and $\mathcal{T}=mT$, respectively, and do not require crossing of quasienergies. We recall that for reaching a sustainable localization, the conditions (a), (b), or (c) have to be complemented with the requirement that the particle does not delocalizes during one evolution cycle $\mathcal{T}$. For the system

under investigation we found (within the analytical approach) that for $T=2t_p$ and pulse amplitudes obeying Eq. (24) the localization mechanism is determined by the condition (b) in which the wave function of the system collapses into a pure Floquet state. In this case we obtained $A_1=0$ ($A_2=0$) for n even (odd) in Eq. (24). For $T\neq 2t_p$ and pulse strengths determined by Eq. (24) we found that the localization mechanism corresponds to the condition (c) and Eq. (26) holds with $\mathcal{T}=2T$. Consequently, a localization condition [equivalent to Eq. (24)] in terms of the quasienergies can be written as

$$\varepsilon_\lambda=\left(n\pm\frac{1}{2}\right)\frac{\hbar\omega_0}{2}. \tag{28}$$

In obtaining Eq. (28) we took into account Eqs. (22) and (23).

The condition in Eq. (28) is represented in Fig. 4 by the intersection of the straight dotted lines with the quasienergies (dashed lines). A comparison of Figs. 1 and 4 confirms that Eq. (28) determines the pulse amplitudes corresponding to optimal localization.

Apart from the conditions (a), (b), and (c), the wave function of the system can be written as in Eq. (26) with $\mathcal{T}=T_c$ in the cases the system dynamics is similar to the field-free case (i.e., when the system behaves as *transparent* to the external field). We have found that this situation occurs if

$$\epsilon_2-\epsilon_1=(1-j)\hbar\omega_0+(2j-1)\hbar\omega_c \tag{29}$$

with $j=0$ or $j=1$. The condition in Eq. (29) does not lead, however, to a sustainable localization, since the localization of the particle within one evolution cycle cannot be guaranteed (note that in this case $\mathcal{T}=T_c$ and the system behaves, essentially, as in the absence of external field). Equation (29) corresponds to avoided crossings of the quasienergies (see Fig. 4) and leads to optimal delocalization, as can be appreciated from the comparison of Figs. 1 and 4 [i.e., Eq. (29) constitutes a delocalization condition, equivalent to Eq. (25) with n odd (even) corresponding to $j=0$ ($j=1$)].

2. The emission spectrum

After performing a procedure similar to that used in Ref. 2, we found that the emission spectrum [Eq. (6)] is determined by

$$I(\omega)=\left|I_1(\omega)+I_2(\omega)+I_3(\omega)\right|, \tag{30}$$

where

$$I_1(\omega)=2\pi\sum_{l=1}^{2}\sum_{m,n=-\infty}^{\infty}\left[\left|A_l\right|^2\int_{-\infty}^{\infty}b_{ln}^*(z)zb_{lm}(z)dz\times\delta((m-n)\omega_0-\omega)\right], \tag{31}$$

$$I_2(\omega)=2\pi A_1A_2^*\sum_{m,n=-\infty}^{\infty}\left[\int_{-\infty}^{\infty}b_{2n}^*(z)zb_{1m}(z)dz\times\delta((m-n)\omega_0+(\epsilon_2-\epsilon_1)/\hbar-\omega)\right], \tag{32}$$

and

$$I_3(\omega)=2\pi A_2A_1^*\sum_{m,n=-\infty}^{\infty}\left[\int_{-\infty}^{\infty}b_{1n}^*(z)zb_{2m}(z)dz\times\delta((m-n)\omega_0+(\epsilon_1-\epsilon_2)/\hbar-\omega)\right]. \tag{33}$$

In Eqs. (31)–(33) A_l represents the expansion coefficients in Eq. (18) and $b_{ln}(z)$ are the coefficients of the Fourier expansion of the lth Floquet mode, i.e.,

$$\Phi_l(z,t)=\sum_{n=-\infty}^{\infty}b_{ln}(z)e^{in\omega_0t};\quad l=1,2. \tag{34}$$

Unlike the case of a cw laser as a driving field, in the present case the coefficients $b_{ln}(z)$ do not have well-defined parity. Therefore, no selection rules for the integrals in Eqs. (31)–(33) can be stated and the emission spectrum is composed, in general, of a static component at $\omega=0$ [corresponding to $m=n$ in Eq. (31)], integer harmonics at $\omega=(m-n)\omega_0$ [corresponding to $m\neq n$ in Eq. (31)], a bandhead at $\omega=(\epsilon_2-\epsilon_1)/\hbar$ [corresponding to $m=n$ in Eq. (32)], and doublets at $\omega=(m-n)\omega_0\pm(\epsilon_2-\epsilon_1)/\hbar$ [corresponding to $m\neq n$ in Eqs. (32) and (33)] around the integer harmonics. One can design the emission spectrum by using Eq. (23) for the estimation of the appropriate pulse parameters.

The emission spectrum (vertical lines represent the emission peaks) obtained through exact numerical calculations for different values of the pulse strength is shown in Fig. 5. The general case in which the four kind of emission lines are present is shown in Fig. 5(a), where the phenomena of low-frequency generation (LFG) is also quite apparent. Because of the absence of accidental degeneration of the quasienergies there is a lower limit for the LFG determined by the lowest value of the difference $\epsilon_2-\epsilon_1$ (note that this lowest value corresponds precisely to the characteristic frequency ω_c of the undriven system), i.e., at the pulse parameters leading to optimal delocalization (see Figs. 1 and 4). Under the condition of optimal delocalization only the line corresponding to LFG (that in this limit coincides with ω_c) survives, while the other lines collapse, i.e., the system behaves as transparent to the external field [see Fig. 5(b)]. On the contrary, when $\epsilon_2-\epsilon_1=\hbar\omega_0/2$, the doublets coincide at odd multiples of $\omega_0/2$. This situation corresponds to the process of optimal localization and the corresponding emission spectrum is displayed in Fig. 5(c), where half-harmonic generation [i.e., at $\omega=n\omega_0/2$ ($n=0,1,2,3,\ldots$)] can be clearly appreciated. As clear from Eq. (17), the large static component present in Fig. 5(c) is a manifestation of the strong localization effects [note also that in the case of optimal delocalization displayed in Fig. 5(b) the static component vanishes].

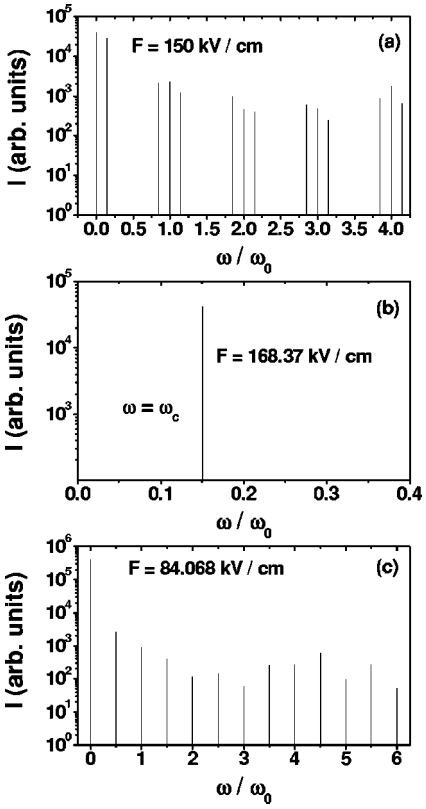

FIG. 5. Emission spectrum for different values of the pulse strength.

B. Optical initial condition

Although the previous case is widely treated in the literature, in practice, the more realistic situation is that the initial state corresponds to the ground state of the field-free system. Therefore, in the present case we consider this particularly important situation. Because of the symmetry of the double-well heterostructure, before applying the pulses, the particle is completely delocalized, with the same probability of being in the left or right well. This situation is represented by the vector (0,0,1) in the Bloch space [note that the vector (0,0,1) actually corresponds to a stationary state, since it is invariant to rotations around the z axis]. On the basis of the analytical approach one can find several strategies for inducing the electron localization with a quasiperiodic train of HCP's. By setting, for example, $T=T_c/4$ and pulse amplitudes such that

$$\frac{2\mu\Delta p}{\hbar}=(4n+1)\frac{\pi}{2} \quad (n\in\mathcal{Z}), \tag{35}$$

the Bloch vector will follow periodically the cycle A-B-C-D-A [here A (B) represents the positive direction of the z (y) axis and C (D) the negative direction of the x (y) axis] and the electron will be localized in the left well. As we are specially interested in the case $T<T_c/4$ we also studied the possibility of inducing electron localization for that case. Following the geometrical interpretation of the evolution of the system one can find (although now the situation is less intuitive) that for $T<T_c/4$ the Bloch vector performs closed

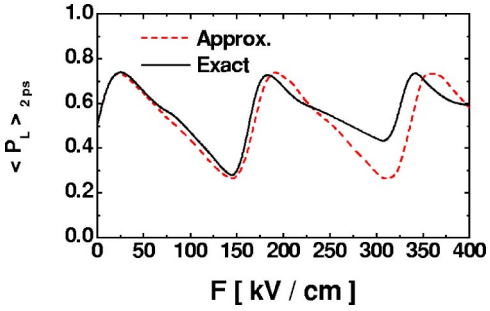

FIG. 6. (Color online) Time average of P_L as a function of the pulse strength for optical initial condition.

circuits corresponding to localization in the left (right) well if the pulse amplitudes obey the relation

$$\frac{2\mu\Delta p}{\hbar}=(2n+1)\frac{\pi}{2}+(-1)^{n+1}\frac{\pi}{4}, \quad n\in\mathcal{Z}, \tag{36}$$

with n even (odd). On the other hand, for $T<T_c/4$ and pulse amplitudes such that

$$\frac{2\mu\Delta p}{\hbar}=n\pi, \quad n\in\mathcal{Z}, \tag{37}$$

the electron will remain delocalized.

The average probability $\langle P_L\rangle_{2\mathrm{ps}}$ as a function of the pulse amplitude is displayed in Fig. 6 for the case $T=100$ fs $<T_c$. Solid and dashed lines correspond to the exact numerical calculations and to the analytical approximation, respectively. It is clear from Fig. 6 that the initially delocalized electron can be steered to one well or to the other by choosing an appropriate value for the pulse amplitudes. A similar effect is achieved by changing the direction of the pulses. The time dependence of the probability of finding the electron in the left well is shown in Figs. 7(a) and 7(b) for pulse

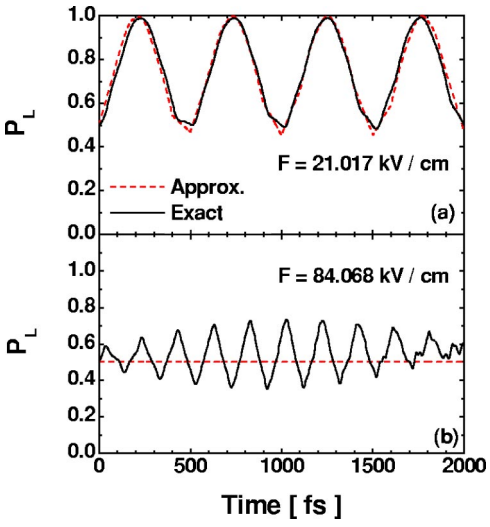

FIG. 7. (Color online) *Optical initial condition*. (a) Time dependence of P_L for a pulse amplitude corresponding to $n=0$ in the localization condition, Eq. (36). (b) Same as in (a) but for a pulse amplitude corresponding to $n=1$ in the delocalization condition, Eq. (37).

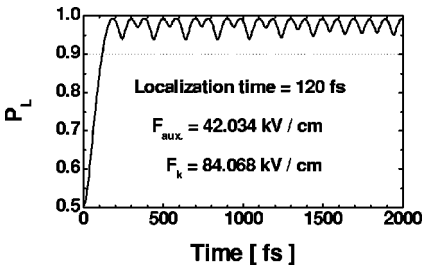

FIG. 8. Optimal localization process for the case of optical initial condition.

amplitudes obeying Eqs. (36) and (37), respectively.

The process of inducing the electron localization of an initially delocalized electron by using a train of uniform quasiperiodic HCP's is not highly efficient (compare Figs. 1 and 6). Therefore we consider the possibility of optimizing the localization process by applying at first an auxiliary HCP and, after an appropriate time delay, a quasiperiodic train of HCP's.

By application of an auxiliary pulse with peak amplitude F_{aux} such that the condition $2\mu\Delta p_{\mathrm{aux}}/\hbar=\pi/2$ holds [this pulse will rotate the Bloch vector from its initial direction (0,0,1) into (0,1,0)] and after a subsequent time delay $\tau=T_c/4+\gamma(\gamma<T_c/4)$, the Bloch vector of the system evolves to the position 1 in Fig. 2. One can then induce a strong localization of the electron in the left well by applying a train of HCP's with period $T\approx 2\gamma$ and obeying the localization condition, Eq. (24). Thus, the first pulse pushes the electron into the left well and the subsequent train of HCP's maintains the particle localization in that well.

The results corresponding to the exact numerical calculations are shown in Fig. 8. One can see from Fig. 8 that strong localization of the initially delocalized electron can be achieved in times of the order of hundreds of femtoseconds. This finding is in sharp contrast to the case when cw lasers are used as driving fields,[2] where it has not been possible to achieve such a strong localization and, in addition, the time needed for the control of the electron motion is found to be on the order of few picoseconds.[2] Thus, the use of HCP's for controlling the electron motion in symmetric double quantum wells can be potentially useful for applications in designing electro-optical devices such as efficient ultrafast switches.

IV. CONCLUSION

In summary, we showed that electron motion in a symmetric double quantum well can be controlled efficiently by applying a train of ultrashort HCP's. An appropriately designed train of HCP's was utilized to control the electron motion in times on the order of hundreds of femtoseconds, a finding which is of relevance for designing ultrafast electro-optic devices. Phenomena such as coherent suppression of tunneling in the absence of accidental degeneration of the quasienergies, low-frequency generation, and half-harmonic generation were discussed. The range of the appropriate pulse parameters for controlling the electron dynamics was determined by means of an approximate analytical model.

[1] F. Grossmann, T. Dittrich, P. Jung, and P. Hänggi, Phys. Rev. Lett. **67**, 561 (1991); J. Gómez Llorente and J. Plata, Phys. Rev. A **45**, R6958 (1992).
[2] R. Bavli and H. Metiu, Phys. Rev. Lett. **69**, 1986 (1992); Phys. Rev. A **47**, 3299 (1993).
[3] T. Mančal and V. May, Eur. Phys. J. D **14**, 173 (2001); M. Grifoni, L. Hartmann, and P. Hänggi, Chem. Phys. **217**, 167 (1997).
[4] R.R. Jones, D. You, and P.H. Bucksbaum, Phys. Rev. Lett. **70**, 1236 (1993); N.E. Tielking and R.R. Jones, Phys. Rev. A **52**, 1371 (1995); N.E. Tielking, T.J. Bensky, and R.R. Jones, *ibid.* **51**, 3370 (1995); R.R. Jones, Phys. Rev. Lett. **76**, 3927 (1996); D. You, R.R. Jones, P.H. Bucksbaum, and D.R. Dykaar, Opt. Lett. **18**, 290 (1993); J.G. Zeibel and R.R. Jones, Phys. Rev. A **68**, 023410 (2003).
[5] M.T. Frey and F.B. Dunning, Phys. Rev. A **59**, 1434 (1999).
[6] B.E. Tannian, C.L. Stokely, F.B. Dunning, C.O. Reinhold, S. Yoshida, and J. Burgdörfer, Phys. Rev. A **62**, 043402 (2000).
[7] C.M. Dion, A. Keller, and O. Atabek, Eur. Phys. J. D **14**, 249 (2001).
[8] A. Matos-Abiague and J. Berakdar, Chem. Phys. Lett. **382**, 475 (2003).
[9] L. Quiroga and N.F. Johnson, Phys. Rev. Lett. **83**, 2270 (1999); P. Zhang and X. Zhao, J. Phys.: Condens. Matter **13**, 8389 (2001).
[10] M. Grifoni and P. Hänggi, Phys. Rep. **304**, 167 (1997).
[11] J. Shao and P. Hänggi, Phys. Rev. A **56**, R4397 (1997).
[12] Y. Dakhnovskii and R. Bavli, Phys. Rev. B **48**, 11 010 (1993).
[13] H. Wang, V.N. Freire, and X. Zhao, Phys. Rev. A **58**, 1531 (1998).
[14] M. Holthaus, Phys. Rev. Lett. **69**, 1596 (1992).
[15] D. You, R.R. Jones, P.H. Bucksbaum, and D.R. Dykaar, Opt. Lett. **18**, 290 (1993); R.R. Jones, Phys. Rev. Lett. **76**, 3927 (1996); J.G. Zeibel and R.R. Jones, Phys. Rev. A **68**, 023410 (2003).
[16] F. Robicheaux, Phys. Rev. A **60**, 431 (1999); O. Zobay and G. Alber, Phys. Rev. **60**, 1314 (1999); C.O. Reinhold, M. Melles, H. Shao, and J. Buegdörfer, J. Phys. B **26**, L659 (1993).
[17] J. Squier, F. Salin, G. Mourou, and D. Harter, Opt. Lett. **16**, 324 (1991); V. Krainov and M.B. Smirnov, Phys. Rep. **370**, 237 (2002).
[18] E. Hertz, N.A. Papadogiannis, G. Nersisyan, C. Kalpouzos, T. Halfmann, D. Charalambidis, and G.D. Tsakiris, Phys. Rev. A **64**, 051801 (2001).
[19] A.E. Kaplan, S.F. Straub, and P.L. Shkolnikov, Opt. Lett. **22**, 405 (1997); V.P. Kalosha and J. Herrmann, Phys. Rev. Lett. **83**, 544 (1999).
[20] A. Wetzels, A. Gürtel, H.G. Muller, and L.D. Noordam, Eur. Phys. J. D **14**, 157 (2001).
[21] G. Bastard, *Wave Mechanics Applied to Semiconductor Heterostructures* (Les Editions de Physique, Les Ulis, 1998).
[22] R. Heather and H. Metiu, J. Chem. Phys. **86**, 9 (1987).
[23] J. von Neumann and E. Wigner, Phys. Z. **30**, 467 (1929).